Origins of luminescence from nitrogen-ion-implanted epitaxial GaAs

X. Weng and R. S. Goldman[a)]
Department of Materials Science and Engineering, University of Michigan, Ann Arbor, Michigan 48109

V. Rotberg
Department of Nuclear Engineering and Radiological Sciences, University of Michigan, Ann Arbor, Michigan 48109

N. Bataiev and L. J. Brillson
Department of Electrical Engineering, Ohio State University, Columbus, Ohio 43210-1272

(Received 21 April 2004; accepted 17 August 2004)

We have examined the origins of luminescence in N-ion-implanted epitaxial GaAs, using a combination of cross-sectional transmission electron microscopy and low-energy electron-excited nanoscale-luminescence spectroscopy. A comparison of reference, as-implanted, and implanted-plus-annealed samples reveals a variety of emissions. In all samples, we observe the GaAs fundamental band-gap emission, as well as several emissions related to GaAs native defects. In the as-implanted and implanted-plus-annealed samples, an emission related to the implantation-induced defects, is also observed. Interestingly, in the implanted-plus-annealed samples, we identify a near-infrared emission associated with GaAsN nanocrystallites. © *2004 American Institute of Physics*. [DOI: 10.1063/1.1803940]

Recently, the controlled nanoscale crystallization of amorphous solids has emerged as a promising means for producing technologically useful nanocomposite materials.[1] In the case of semiconductors, the controlled formation of crystalline structures on the nanoscale provides an opportunity for producing new materials with unique electronic and optical properties. For example, a continuous buried layer of wurtzite GaN nanocrystals was produced by N ion implantation into a GaAs substrate, followed by furnace annealing.[2] We recently showed that a buried layer of nitrogen-rich GaAsN nanocrystallites within an apparently amorphous matrix may be synthesized by N ion implantation into epitaxial GaAs followed by rapid thermal annealing (RTA).[3] Furthermore, we find that high-temperature RTA induces simultaneous blistering of the GaAsN nanostructure layer, which may provide a new opportunity for the integration of the nanostructure layer with a variety of substrates.[4] A detailed understanding of the optical properties is critical for potential applications of the ion-beam-synthesized GaAsN nanocrystallites. In an earlier report,[3] photoluminescence (PL) measurements showed significant near-infrared emission from implanted-plus-annealed epitaxial GaAs samples, presumably associated with the GaAsN nanostructures. Here, we report on the origins of luminescence from nitrogen-ion-implanted epitaxial GaAs, using a combination of cross-sectional transmission electron microscopy (TEM) and depth-resolved low-energy electron-excited nanoscale-luminescence (LEEN) spectroscopy.[5] We observe the emission from GaAs fundamental band-gap transition, as well as emissions from native defects in GaAs. We also observe an emission apparently related to implantation-induced defects. Interestingly, we reveal a near-infrared emission associated with the ion-beam-synthesized GaAsN nanostructures.

For these studies, $\sim$2-μm-thick *n*-doped GaAs films grown by molecular-beam epitaxy on (001) GaAs were implanted with nitrogen at an incident ion energy of 100 keV and a nominal dose of 5×10^{17} cm^{-2}, as described in an earlier report.[3] Some of the implanted samples were subsequently rapid thermal annealed in argon gas at 800 °C for 30 s. Cross-sectional TEM specimens were prepared using conventional mechanical polishing, followed by argon ion milling at 77 K. TEM imaging and electron diffraction were carried out in a JEOL 4000EX operating at 400 kV.

LEEN analysis was performed using a JEOL 7800F ultrahigh vacuum (UHV) scanning electron microscope with an Oxford liquid-helium-cooled sample stage. Luminescence from carrier recombination was collected using an Oxford MonoCL apparatus, consisting of a parabolic mirror on the UHV side coupled through a sapphire view port to an air side photomultiplier tube and monochromator with maximum spectral resolution of 0.15 nm. LEEN spectra were measured from 800 to 1550 nm at 10 K. The depths of excitation for different electron-beam energies (E_B) were predicted using a CASINO Monte Carlo simulation.[6] Based on the simulation results, E_B was varied from 5 to 15 keV in order to obtain emissions from different layers of the samples.

Typical dark-field diffraction contrast TEM images of (a) as-implanted and (c) implanted-plus-annealed samples are shown in Fig. 1. These images were obtained using the GaAs 004 beam and when possible, a portion of the diffraction ring closest to the GaAs 004 spot. Both TEM images show evidence of three regions: (1) a $\sim$100-nm-thick surface layer, (2) a $\sim$150-nm-thick middle layer, and (3) a near-substrate layer. The corresponding diffraction patterns, shown in Figs. 1(b) and 1(d), respectively, were collected from an area including all three layers. For the as-implanted sample shown in Fig. 1(a), the middle layer appears opaque, suggesting that it is essentially amorphous. This is also indicated by the selected area diffraction (SAD) pattern shown in Fig. 1(b), which contains both diffraction spots associated with GaAs, and a diffuse ring presumably due to the apparently amorphous middle layer. For the 800 °C annealed sample shown in Fig. 1(c), the middle layer contains a high density of

[a)]Author to whom correspondence should be addressed; Email address: rsgold@engin.umich.edu

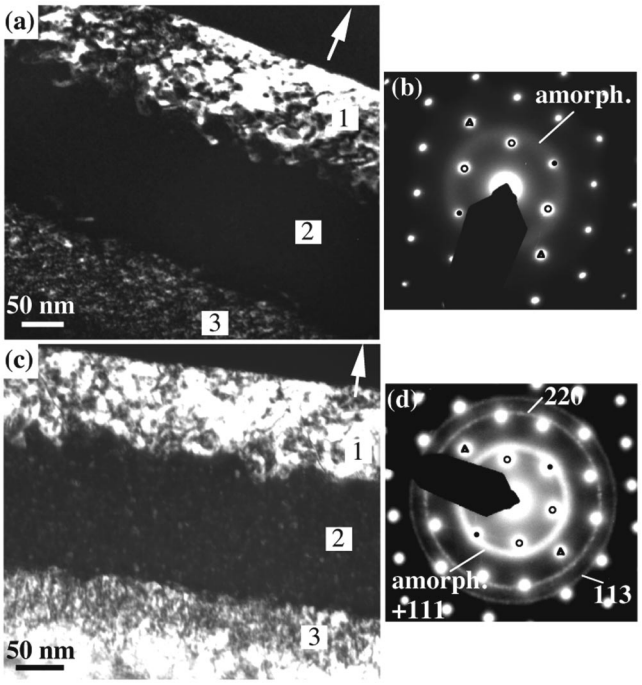

FIG. 1. Dark-field TEM images of (a) as-implanted and (c) implanted plus 800 °C annealed samples, obtained using the GaAs 004 beam, and when possible, a portion of the crystallite 113 diffraction ring closest to the GaAs 004 spot. The direction of the arrow in each figure is ⟨004⟩. (b) and (d) are the SAD patterns corresponding to (a) and (c), respectively. The major diffraction spots from the crystalline GaAs {111}, {220}, and {002}, are indicated by circles, triangles, and black dots, respectively. The regions labeled 1, 2, and 3 indicate the surface, middle, and near-substrate layers, respectively.

nanometer-sized circular bright features, suggesting the formation of nanocrystallites. The SAD pattern in Fig. 1(d) contains three spotty rings associated with the nanocrystallites, in addition to the GaAs diffraction spots and the diffuse ring. The interplanar spacings corresponding to these three rings are 2.61 ± 0.01, 1.60 ± 0.01, and 1.37 ± 0.01 Å, respectively. These are within 1% of the {111}, {220}, and {l13} interplanar d spacings of pure zincblende GaN, suggesting the formation of GaN-rich GaAsN crystallites. High-resolution TEM and x-ray diffraction results also suggested the formation of GaAsN crystallites in implanted-plus-annealed samples.[3] Evidence of the formation of GaAs-rich crystalline phases is not observed, suggesting the preferential formation of GaN-rich crystalline phases over GaAs-rich crystalline phases. Indeed, the formation of GaN-rich crystalline phases is thermodynamically favored due to its lower free energy of formation compared to that of GaAs-rich crystalline phase.[2,7]

The CASINO Monte Carlo simulations are presented in Fig. 2. For electron-beam energies, E_B, of 5, 7, 10, and 15 keV, the positions of maximum energy-loss rates, which correspond to depths of peak excitation of free-electron-hole pair generation, are predicted to be approximately 80, 150, 270, and 470 nm, respectively. As shown in Fig. 1, the surface and middle layers of the as-implanted and implanted-plus-annealed samples are ~100 and 150-nm thick, respectively. Therefore, LEEN spectra collected using 5 and 7 keV electrons are predicted to reveal emissions predominantly from the surface and middle layers in implanted samples, respectively. On the other hand, spectra obtained using $\geqslant$10 keV electrons are predicted to reveal emissions mainly from the near-substrate layer. However, due to the peak

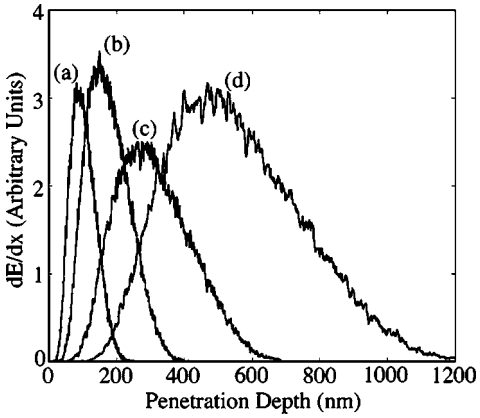

FIG. 2. The variation of the energy loss rate, dE/dx, as a function of penetration depth of (a) 5, (b) 7, (c) 10, and (d) 15 keV electrons incident into GaAs, predicted by CASINO Monte Carlo simulation. Here, dE/dx is normalized to the total energy of the beam divided by the number of electrons participating in the simulation, in order to accommodate multiple simulations with different incident energies and power on the same graph.

broadening at high E_B, emissions from the middle layer may also appear in spectra obtained using $\geqslant$10 keV electrons.

Figure 3 shows LEEN spectra of (a) unimplanted reference, (b) as-implanted, and (c) implanted plus 800 °C annealed samples, collected at electron incident energies ranging from 5 to 15 keV. The spectra of the unimplanted reference sample, shown in Fig. 3(a), are dominated by an emission near 1.47 eV, due to the fundamental band-gap transition of GaAs. For the as-implanted sample, the 1.47 -eV emission is only observed for $E_B > 10$ keV, due to the highly defective nature of the surface, middle, and near-substrate layers of the as implanted sample, as indicated in Fig. 1(a). After RTA, a weak 1.47-eV emission was detected with $E_B \geqslant 10$ keV, suggesting that the defects were partially annealed out in the near-substrate layer. The absence of the 1.47-eV emission for $E_B = 5$ keV suggests the surface layer remains highly defective after RTA, as evidenced by the cross-sectional TEM image in Fig. 1(c).

In the spectra of the unimplanted reference sample shown in Fig. 3(a), three additional emissions near 0.83, 1.02, and 1.33 eV, are also apparent. These emissions are likely related to the M7, M4, and M1 deep levels, respectively, which are often observed in MBE-grown n-GaAs,[8] and are likely associated with Ga vacancies or Ga vacancy-related complexes.[9] The 1.33-eV emission is not observed in the spectra of the as-implanted sample shown in Fig. 3(b), suggesting that the emission has been quenched by the implantation-induced defects. For the implanted-plus-annealed sample, the 1.33-eV emission is apparent in spectra collected with $E_B \geqslant 8$ keV, as shown in Fig. 3(c). Since the LEEN spectra with $E_B = 8$ keV reveal emissions predominantly from the near-substrate layer, the recovery of the 1.33-eV emission at $E_B = 8$ keV suggests that the RTA process reduces the concentration of implantation-induced defects in the near-substrate layer. On the other hand, the concentration of implantation-induced defects in the surface layer apparently remains high enough to quench the 1.33 -eV emission for $E_B = 5$ keV. A weak peak near 0.92 eV is also apparent in the spectra from the as-implanted sample shown in Fig. 3(b). Careful examination of spectra in Figs. 3(a) and 3(c) suggests that this emission also appears as a shoulder of 1.02-eV emission in the as-implanted and

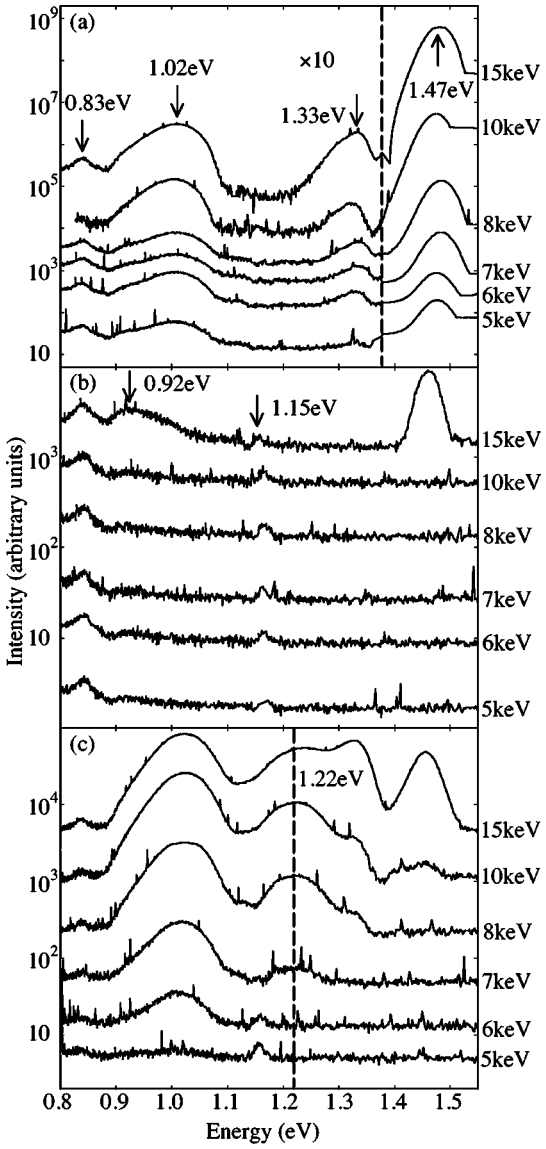

FIG. 3. LEEN spectra of (a) unimplanted reference, (b) as-implanted, and (c) implanted plus 800 °C annealed samples, collected at electron excitation energies ranging from 5 to 15 keV. In (a), the data points to the left of the vertical dashed line have been multiplied by 10. In (d), the vertical dashed line indicates the ~1.22 eV emission emerged after annealing.

implanted-plus-annealed samples. Thus, 0.92 eV is apparently related to native defects of GaAs, rather than implantation-induced defects. Indeed, it may be related to the M5 deep level in MBE-grown *n*-GaAs, which is also likely associated with Ga vacancies.[8,9]

In the spectra from the as-implanted and implanted-plus-annealed samples in Figs. 3(b) and 3(c), an emission at ~1.15 eV is also apparent. This emission was also observed by deep level transient spectroscopy measurements in nitrogen-ion-implanted GaAs doses ranging from 1×10^{12} to 2×10^{15} cm^{-2},[10,11] and is likely related to the implantation-induced $E3$ defects.[12] Apparently, such defects cannot be fully removed by RTA at 800 °C for 30 s.

Interestingly, in the spectra for the implanted-plus-annealed sample, an emission at ~1.22 eV is evident for $E_B \geqslant 7$ KeV. This emission is not observed in either the reference or the as-implanted sample, and cannot be accounted for by any native or irradiation-induced defects of GaAs.[8–12] These results strongly suggest that the 1.22-eV emission originates from the GaAsN nanocrystallites in the middle layer. The appearance of this emission in spectra collected with $\geqslant$10 keV electrons is likely a result of the broadening of the electron excitation, as shown in Fig. 2. The difference in energy between this 1.22-eV emission and the GaAs 1.47-eV emission is ~0.25 eV in LEEN spectra shown in Fig. 3. In our earlier PL measurements on the implanted-plus-annealed samples, we observed an emission near 1.27 eV, which had an energy difference of ~0.23 eV with respect to the 1.5-eV GaAs emission.[3] Thus, it is likely that the 1.22-eV emission observed in LEEN corresponds to the emission near 1.27 eV observed in PL. Assuming that the 1.22-eV emission corresponds to a fundamental band-gap transition, the band-gap energy of the GaN-rich GaAsN nanocrystallites is significantly smaller than that of bulk zincblende GaN (3.3 eV).[13] It has been predicted that the incorporation of ~4.5 at.% As into GaN lowers the band gap to ~1.22 eV.[14] Using a linear interpolation of GaAs and GaN lattice parameters, this corresponds to an alloy, $GaAs_{0.09}N_{0.91}$, with a lattice parameter of 4.60 Å, within 2.0% of our electron-diffraction results and 1.5% of our x-ray diffraction results.[3] Therefore, the apparent lowering of the fundamental band gap of the GaAsN nanocrystallites is likely due to the incorporation of a small amount of As in GaN. Overall, these results illustrate the potential for ion-beam-synthesis of light-emitting GaAsN nanocrystallites.

This work at the University of Michigan (UM) was supported in part by the UM Office of the Vice President for Research Initiative in Materials Research Grant; the DOD Multidisciplinary University Research Initiative, administered by the Air Force Office of Scientific Research; the Department of Energy (DOE), through the National Renewable Energy Laboratory Photovoltaics Beyond the Horizon Program; and the TRW Foundation. We also acknowledge the assistance of the staff of the Michigan Ion Beam and the Electron Microbeam Analysis Laboratories at UM. The work at Ohio State University was supported in part by the DOE, NSF, and the Office of Naval Research.

[1] A. Meldrum, R. F. Haglund Jr., L. A. Boatner, and C. W. White, Adv. Mater. (Weinheim, Ger.) **13**, 1431 (2001).
[2] X. W. Lin, M. Behar, R. Maltez, W. Swider, Z. Liliental-Weber, and J. Washburn, Appl. Phys. Lett. **67**, 2699 (1995).
[3] X. Weng, S. J. Clarke, W. Ye, S. Kumar, R. S. Goldman, A. Daniel, R. Clarke, J. Holt, J. Sipowska, A. Francis, and V. Rotberg, J. Appl. Phys. **92**, 4012 (2002).
[4] X. Weng, W. Ye, R. S. Goldman, and J. C. Mabon, J. Vac. Sci. Technol. B **22**, 989 (2004).
[5] L. J. Brillson, J. Vac. Sci. Technol. B **19**, 1762 (2001).
[6] P. Hovington, D. Drouin, and R. Gauvin, Scanning **19**, 1 (1997).
[7] X. Weng, Ph.D. thesis, University of Michigan, 2003, pp. 239–240.
[8] D. V. Lang, A. Y. Cho, A. C. Gossard, M. Ilegems, and W. Wiegmann, J. Appl. Phys. **47**, 2558 (1976).
[9] P. K. Bhattacharya and S. Dhar, in *Semiconductors and Semimetals*, Vol. 26, edited by R. K. Willardson and A. C. Beer (Academic, San Diego, 1988), p. 143.
[10] J. F. Chen, J. S. Wang, M. M. Huang, and N. C. Chen, Appl. Phys. Lett. **76**, 2283 (2000).
[11] P. Jayavel, K. Santhakumar, and K. Asokan, Nucl. Instrum. Methods Phys. Res. B **212**, 496 (2003).
[12] D. V. Lang, Inst. Phys. Conf. Ser. **31**, 70 (1977).
[13] M. Leroux and B. Gil, in *Properties, Processing and Applications of Gallium Nitride and Related Semiconductors*, edited by J. H. Edgar, S. T. Strite, I. Akasaki, H. Amano, and C. Wetzel (INSPEC, London, UK, 1999), p. 45.
[14] L. Bellaiche, S.-H. Wei, and A. Zunger, Phys. Rev. B **54**, 17568 (1996).